

Diaza crown-type macromocycle (kryptofix 22) functionalised carbon nanotube for efficient Ni²⁺ loading; A unique catalyst for cross-coupling reactions

Michael Aalinejad^a, Nader Noroozi Pesyan^{a,*}, Esmail Doustkhah^{b,*}

^a Department of Organic Chemistry, Faculty of Chemistry, Urmia University, 57159, Urmia, Iran

^b International Center for Materials Nanoarchitectonics (MANA), National Institute for Materials Science (NIMS), 1-1 Namiki, Tsukuba, Ibaraki, 305-0044, Japan

ARTICLE INFO

Keywords:

Carbon nanotube
C–C coupling
–CN coupling
–CO coupling
Kryptofix 22
4,13-diaza-18-crown-6

ABSTRACT

Raising the capability of supporting and suppressing the leaching possibility to a very insignificant level has still remained challenging for some class of transition metals, i.e. Ni²⁺. Here we present the covalent functionalisation of macrocyclic ligand, 4,13-diaza-18-crown-6 (kryptofix 22), on the surface of carbon nanotube (CNT), leading to a unique adsorptive capability for supporting Ni²⁺. This material was incorporated as a promising catalyst in coupling reactions including C–C, CN, and CO— cross-coupling reactions. We demonstrate that the kryptofix 22 functionalisation on the surface of CNT has a key role in the enhancement of the adsorption capability Ni²⁺ and subsequent catalytic activity. We further prove that this ligand causes a significant boost in the recyclability of the reactions due to the extremely trivial Ni²⁺ leaching from the CNT's surface during the reactions.

1. Introduction

Nanoarchitecture of carbon-based materials toward a unique and smart heterogeneous catalyst has acquired a significant attention in recent years toward green chemical processes [1–4]. Heterogeneous catalysts, among them, with transition metal basis as the frontiers of green catalysis for chemical processes have granted many breakthroughs in the field [5–8], however, several transition metal ions like Ni²⁺ are suffering from the high efficiency being efficiently loaded on the surface with insignificant leaching [9–14]. Therefore, researches to develop the textural ability of a heterogenous surface for a stronger bonding to the metal ions are still ongoing. Among the candidates, pure carbon-based materials can have only some weak bonding or interactions with most metal ions and therefore, lead to an inefficient catalyst due to low loading capacity and high leaching possibility [15–17]. However, bearing in mind that some of carbon materials (e.g. CNT) have a high surface area, stability and potential in surface modification [18,19], it can easily convert to an exceptional material through modifying the surface [16,20–25]. Therefore, we aimed to design a catalyst based on CNT with subsequent modification toward a Ni²⁺ supported catalyst.

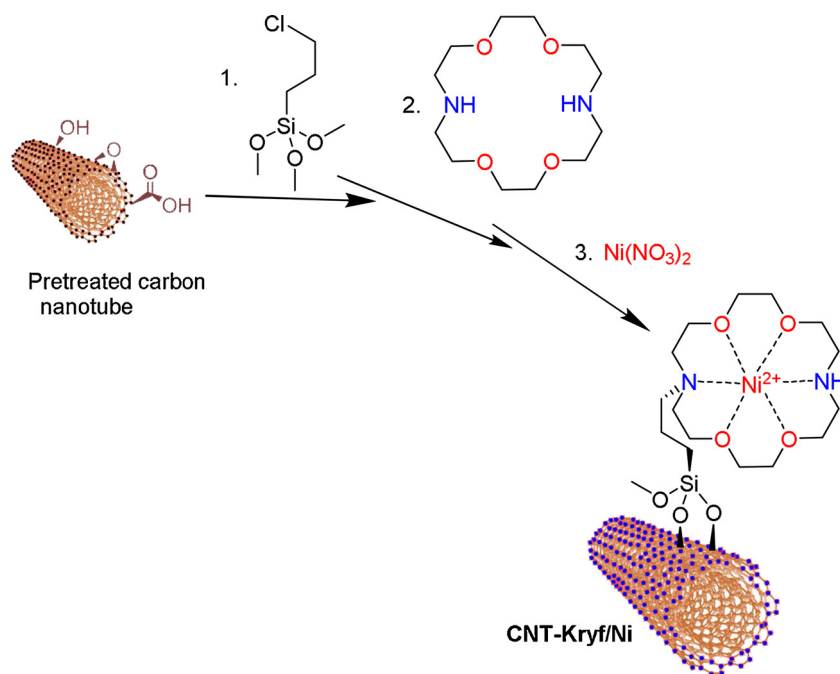
On the basis of previous reports, crown ether macrocyclic compounds have an excellent capacity toward adsorption of metal ions,

even gaseous compounds [26–28]. Therefore, we used kryptofix 22 to functionalise the surface of CNT to reinforce the surface loading capability. Kryptofix 22 is a highly potential macrocyclic compound for incorporating in variety of applications due to its strong complexation capability [29–31]. This macrocyclic compound can compose an organometallic complex with a broad number of metal ions by wrapping and surrounding the metal with several nitrogen and oxygen atoms [31]. Therefore, kryptofix 22 is expectable to have a high capacity in loading metal ions and therefore, it is a promising candidate to be functionalised on a heterogeneous surface to act as a ligand. The use of Ni species as catalyst can be of great importance since Ni is a great alternative to precious metals for coupling reactions from viewpoint of cost-efficiency.

In this work, we designed a catalyst by modifying the CNT surface with kryptofix 22 to enhance the Ni²⁺ loading capacity [32], and subsequent rise in the catalytic activity in the recyclability. This catalyst was incorporated in the cross coupling of Ph₃SnCl with three different species including aromatic amine (C–N coupling), aromatic halides (C–C coupling), and phenols (C–O coupling). We present a catalyst high stability, surface area and recyclability for coupling reactions.

* Corresponding authors.

E-mail addresses: n.noroozi@urmia.ac.ir (N.N. Pesyan), Doustkhah.esmail@nims.go.jp (E. Doustkhah).



Scheme 1. Synthesis of CNT-Kryf/Ni.

2. Result and discussion

2.1. Catalyst synthesis and characterisation

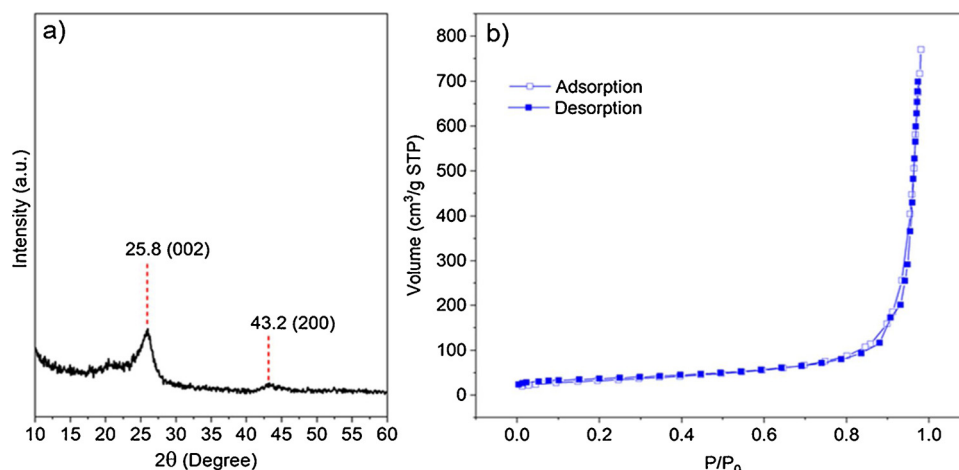
Here, we modified CNT with a kryptofix 22 to obtain a unique surface functionality for supporting Ni^{2+} which is, in turn, difficult to load on a surface. For this, we pretreated the surface with $\text{HNO}_3/\text{H}_2\text{SO}_4$ to generate plenty of hydroxyl and epoxide groups on the surface. The generated hydroxyl groups contribute the surface of CNT to be well-functionalised with CPTMS. Functionalisation of CPTMS decorates the surface with alkyl chloride which subsequently can be incorporated for post-functionalisation with kryptofix 22 (CNT-Kryf). Eventually, we loaded CNT-Kryf with Ni^{2+} to reach an organometallic based heterogeneous catalyst (CNT-Kryf/Ni). Scheme 1 presents a simplified step of CNT-Kryf/Ni.

X-ray diffraction (XRD) pattern of CNT-Kryf/Ni is presented in Fig. 1a. According to the XRD pattern, two characteristic peaks were found at 25.8° and 43.2° which correspond to the (002) and (200) planes. N_2 adsorption-desorption isotherm of CNT-Kryf/Ni was measured and studied. According to the obtained isotherm and Brunauer-

Emmett-Teller (BET) plot CNT-Kryf/Ni has $1.210 \text{ m}^2 \cdot \text{g}^{-1}$ as surface area (Fig. 1b), which is significantly a high surface area. This observation also reveals that the surface area of CNT is not collapsed by several modification and pretreatment steps in comparison with the pristine types of CNT [33,34].

The loading amount of Ni in CNT-Kryf/Ni using ICP-OES found to be 1.30 wt%. The morphology of CNT-Kryf/Ni according to the scanning electron microscopy (SEM) reveals that the CNT parent morphology is retained, as shown in Fig. 3. SEM-mapping and EDS demonstrated the related elements (C, Si, N, O, and Ni) of CNT-Kryf/Ni dispersed throughout the structure (Fig. 2).

The Fourier transform infrared (FT-IR) spectra were obtained at various steps of catalyst synthesis (Fig. 4b). Accordingly, a peak at 1104 cm^{-1} could be attributed to the C–C bond vibration of CNT. The existing peaks at 2761.42 and 2831.52 cm^{-1} could be due to the CH–stretching vibration peak of Kryptofix 22 and n-propyl aliphatic chain. A band at 3438 cm^{-1} is assignable to the stretching vibration of the O–H groups. Appearing some peaks around $1636\text{--}1676 \text{ cm}^{-1}$ after functionalisation of CNT with kryptofix 22 confirms the covalent bonding of kryptofix 22 to the surface of CNT. Raman spectroscopy

Fig. 1. (a) Wide-angle XRD pattern and (b) N_2 adsorption-desorption isotherm of CNT-Kryf/Ni.

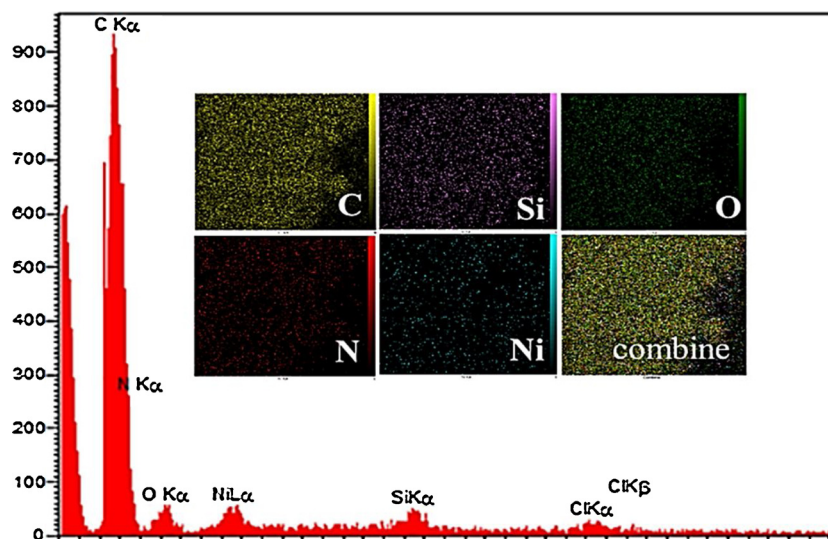


Fig. 2. The EDX spectrum and elemental maps of C, O, Si, N and Ni of CNT-Kryf/Ni.

exhibits the hybridization of ratio of ordered and disordered carbons. Accordingly, D band at 1313 cm^{-1} and G band at 1604 cm^{-1} can be attributed to the ordered and disordered carbon in CNT. Since the D band has higher intensity and arises from defects of carbons, the structure of carbon in CNT-Kryf/Ni is dominantly oxidised in the pre-treatment step (Fig. 4a).

2.2. Catalytic tests

2.2.1. -CC coupling reaction

In this step, CNT-Kryf/Ni as a heterogenous catalyst was tested and examined in different Stille coupling reactions (e.g. C–C, CN and CO—). Therefore, it was examined in the reaction of Ph_3SnCl with aryl iodide to find out an efficient solvent and base, and an optimum temperature to obtain a high yield (Scheme 2). Initially, we used different amounts of catalyst to specify the optimum amount of catalyst. The coupling reaction in the absence of catalyst did not have a tangible progress, while in the presence of the CNT-Kryf/Ni (7 mg) the reaction yielded a significant product (Scheme 2). Among different bases, such as *N*-methylmorpholine, Et_3N and K_2CO_3 , the more effective base in this coupling reaction was K_2CO_3 . Seeking for an optimum temperature in this reaction showed us that the reaction can efficiently proceed at room temperature and raising the temperature is not an essential task. This reaction was checked using several solvents including EtOAc,

dimethylformamide, poly ethylene glycol, CH_2Cl_2 and *N*-methyl pyrrolidone and high yield was obtained by PEG (Fig. 5). The reaction of aryl iodide with Ph_3SnCl in the presence of PEG as solvent, CNT-Kryf/Ni as catalyst was efficiently proceeded at room temperature via a C–C cross coupling. Then, the catalytic capability of other aryl halide derivatives with Ph_3SnCl was tested under the optimum conditions and the results are summarised in Table 1.

Since the Stille C–C coupling reaction is an organometallic based reaction, the mechanism can be also assumed as part of C–C coupling reaction in which the metal species in the first step undergoes oxidative addition to Ph_3SnCl and in the second step, the formed Ni complex 1 bears a transmetalation with Ph-Br to form complex 2. Eventually the complex undergoes a reductive elimination and product 3 is obtained and the Ni-L (L is indicative of CNT-Kryf) regenerates.

2.2.2. -CN coupling reaction

C–N coupling is one of the most important reactions for synthesis of vital intermediates of chemicals and pharmaceutical compounds [32,35]. Therefore, after a successful test on the synthesis of different biphenyl compounds over the catalysis of CNT-Kryf/Ni, the catalytic activity of CNT-Kryf/Ni was examined in C–N cross coupling reaction (Scheme 3). For optimizing the reaction conditions, aniline with Ph_3SnCl was selected as a model reaction in the presence of the catalyst. The experiments demonstrate that using Et_3N as base and PEG as

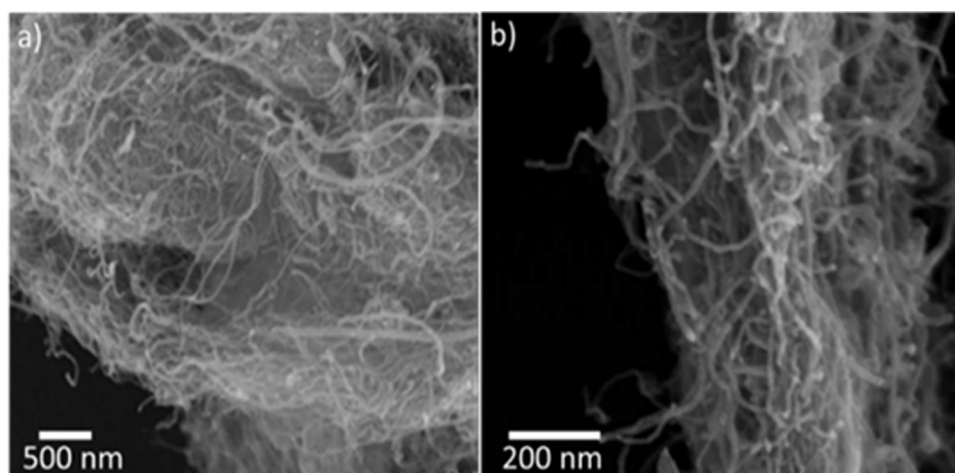


Fig. 3. a) Low and b) high magnification SEM images of CNT-Kryf/Ni.

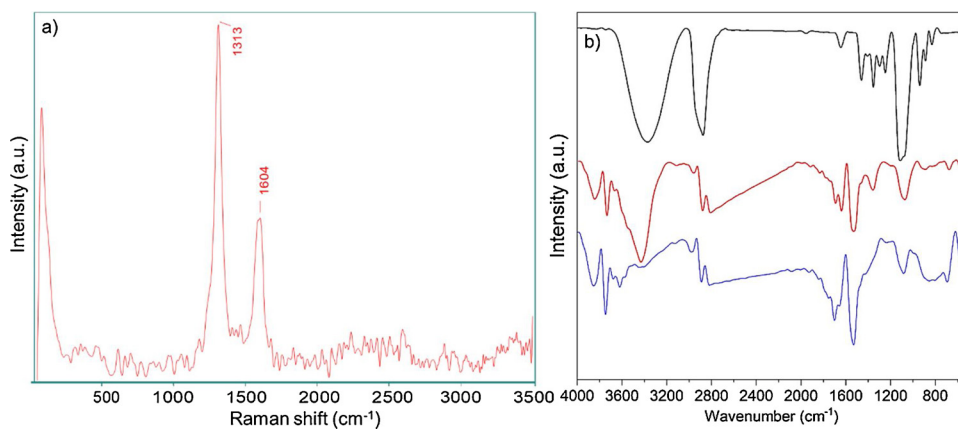


Fig. 4. a) The Raman spectrum of CNT-Kryf/Ni, b) FT-IR spectra of CNTs (black), CNT-Kryf (red), and CNT-Kryf/Ni (blue). (For interpretation of the references to colour in this figure legend, the reader is referred to the web version of this article).

solvent at 95 °C results in C–N bond formation in a very high yield (Table 2, entry 2). Likewise, this reaction was also activated at higher temperature like other many reactions [36]. The reaction of Ph_3SnCl was further successfully applied for several other amines, as summarised in Table 3, either the derivatives with electron-withdrawing groups or electron-donating groups. Comparing the catalytic activity of CNT-Kryf/Ni with CNT/Ni reveals that the presence of kryptofix 22 has a key role in the improvement of the catalytic activity of Ni^{2+} . This is due to the high loading capacity of CNT-Kryf rather than pure CNT.

For discovering the role of kryptofix 22 in the catalytic activity of Ni, the C–N coupling reaction was tested under the identical conditions but with unmodified Ni supported CNT (CNT/Ni). The lower yield and TON of the reaction when catalysed by CNT/Ni reveals the constructive effect of the modification with kryptofix in the improvement of catalytic activity (Scheme 3).

2.2.3. –CO coupling reaction

In this reaction, to gain the optimal reaction conditions of C–O cross coupling reaction, phenol with Ph_3SnCl was tested under the catalysis of CNT-Kryf/Ni. Therefore, we tested different solvents, bases, temperatures and ratios of CNT-Kryf/Ni to reactants. Under the optimal conditions, the reaction in the presence of Et_3N (as base) and PEG (as solvent) at 95 °C for 24 h was found to be more efficient than other evaluated conditions. The reactions of different phenol derivatives with Ph_3SnCl were studied also investigated and we found the same excellent results of this catalyst under the optimal conditions for other derivatives of the reactant (Table 4). We also loaded the Ni^{2+} directly on the

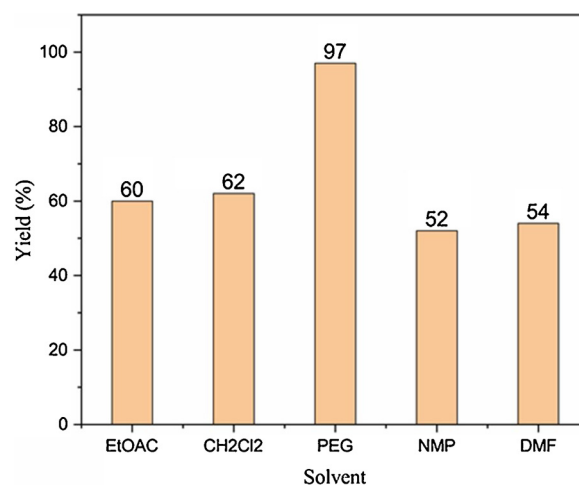
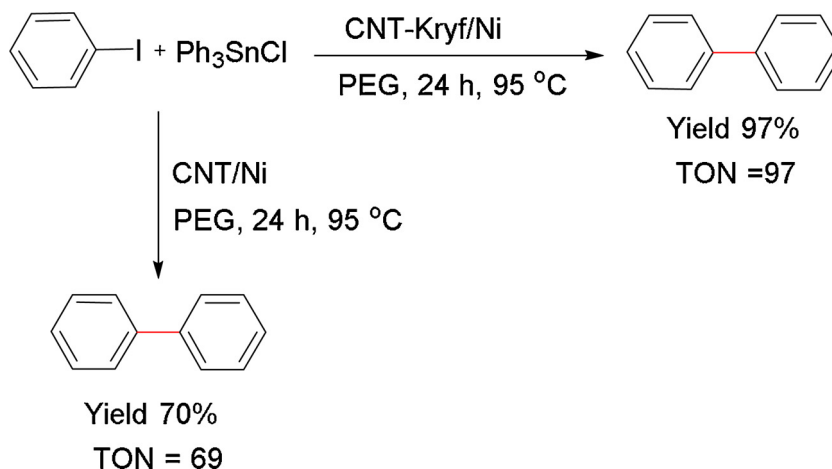


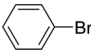
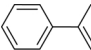
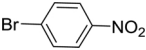
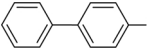
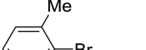
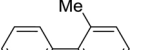
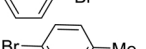
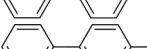
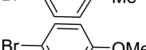
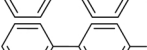
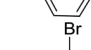

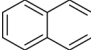
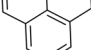
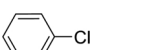
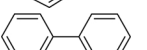
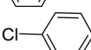
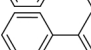
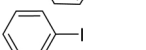
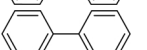
Fig. 5. Solvent influence on C–C coupling reaction of iodobenzene with PhSnCl_3 through the catalysis of CNT-Kryf/Ni.

unmodified CNT, but pretreated with concentrated acid, and repeated the reaction of phenol with Ph_3SnCl . We found that the reaction yield significantly drops when the surface of CNT is not functionalised with kryptofix 22 (CNT/Ni). This comparison reveals the excellence of kryptofix 22 on enhancing the catalytic activity through the enhancing the Ni^{2+} loading capacity (Scheme 4). We also found that the TON of



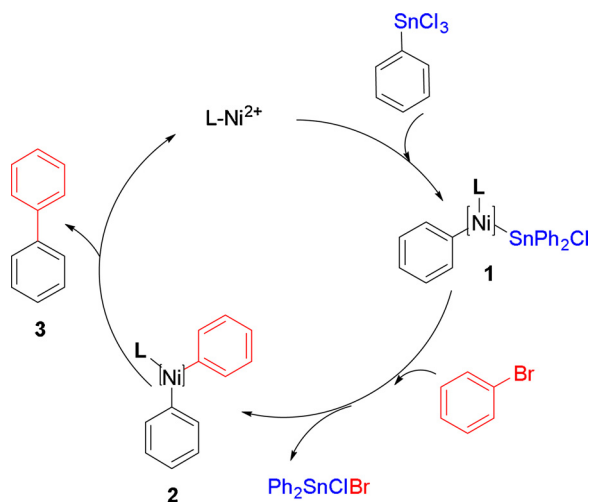
Scheme 2. C–C cross-coupling reaction of iodobenzene with Ph_3SnCl under the catalysis of CNT Kryf/Ni or CNT/Ni under the identical conditions. (Reaction conditions: 1 mmol iodobenzene, 0.5 mmol of Ph_3SnCl and 2 mmol of K_2CO_3 in 2 mL of solvent).

Table 1
Coupling of aryl halides with Ph_3SnCl catalyzed by CNT-Kryf/Ni at room temperature.

$\text{Ar-X} + \text{Ph}_3\text{SnCl} \xrightarrow[\text{PEG, 24 h, rt}]{\text{CNT-Kryf/Ni}} \text{Ar-Ar}'$					
Entry	Aryl halide	Product ^a	Yield (%) ^b	TON	
1			94	93	
2			95	95	
3			90	90	
4			92	92	
5			93	92	
6			86	84	
7			90	90	
8			92	92	
9			97	97	
10			95	95	

^a The products were characterised and identified by comparison of their spectral and physical data with those of authentic samples.

^b Isolated yield.



Scheme 3. Schematic representation of C–C coupling mechanism through the catalysis of CNT-Kryf/Ni.

reaction under the catalysis of CNT-Kryf/Ni is higher than that of CNT/Ni). This observation also demonstrates the kryptofix 22-Ni^{2+} complexation leads to an enhancement in the catalytic activity of the Ni^{2+} (Schemes 4 and 5).

2.2.4. Recyclability and catalytic potential of CNT-Kryf/Ni

Since the heterogeneity of the catalysts are important because of the recyclability and preventing the release of chemicals and toxic materials to the environment [37]. We finally compared the catalytic activity of CNT-Kryf/Ni in all three reactions with previously reported catalysts and realised that CNT-Kryf/Ni acts as a competitive catalyst

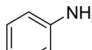
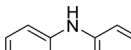
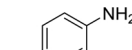
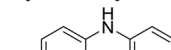
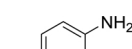
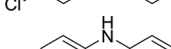
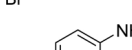
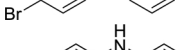
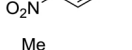
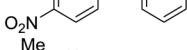
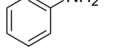
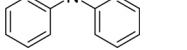
Table 2
Optimisation of parameters for C–N coupling reaction catalyzed by CNT-Kryf/Ni.

Entry ^a	Solvent	Base	Temp (°C)	Time (h)	Yield (%) ^b
1	PEG	Et_3N	95	24	–
2	PEG	Et_3N	95	11	97
3	PEG	Et_3N	95	10	90
4	CH_2Cl_2	Et_3N	Reflux	20	50
5	EtOAc	Et_3N	Reflux	20	55
6	–	Et_3N	r.t.	22	85
7	DMF	Et_3N	95	20	65
8	PEG	Et_3N	r.t.	16	60
9	PEG	Et_3N	65	14	82
10	PEG	K_2CO_3	95	24	–

^a Reaction conditions: 1 mmol of aniline, 7 mg catalyst, 0.5 mmol of Ph_3SnCl and 2 mmol of Et_3N in 2 ml of solvent.

^b Isolated yield.

Table 3
Coupling of amines with Ph_3SnCl catalysed by CNT-Kryf/Ni at 95 °C.

Entry	Amine	Product ^a	Yield (%) ^b	TON
1			97	97
2			86	86
3			91	90
4			95	95
5			70	70
6			78	76

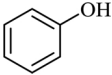
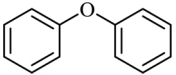
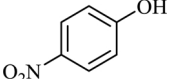
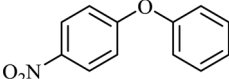
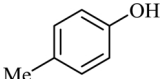
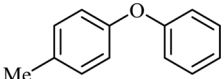
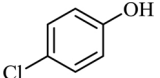
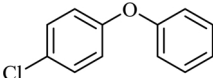
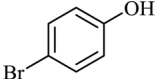
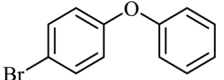
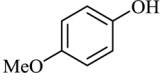
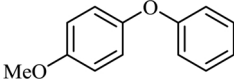
^a The products were recognised and characterised by comparison of their spectral and physical data with those of authentic samples.

^b Isolated yield.

compared to previously reported catalysts [38]. Table 5 reveals that the catalysis of CNT-Kryf/Ni results in a superior or competitive activity compared to the previously reported literatures in the identical reaction. Eventually, the recyclability of the CNT-Kryf/Ni was further studied for all three cross coupling reactions. As a result, recycling the CNT-Kryf/Ni in the reaction of Ph_3SnCl with any of aryl halide, aniline and phenol under the related optimum reaction conditions. As shown in Fig. 6, the CNT-Kryf/Ni was reused for seven consecutive cycles without a significant loss in the catalytic efficiencies. Based on ICP-OES measurements, the leaching of Ni from the catalyst's matrix to the solution after seven cycles was negligible (1.30 %).

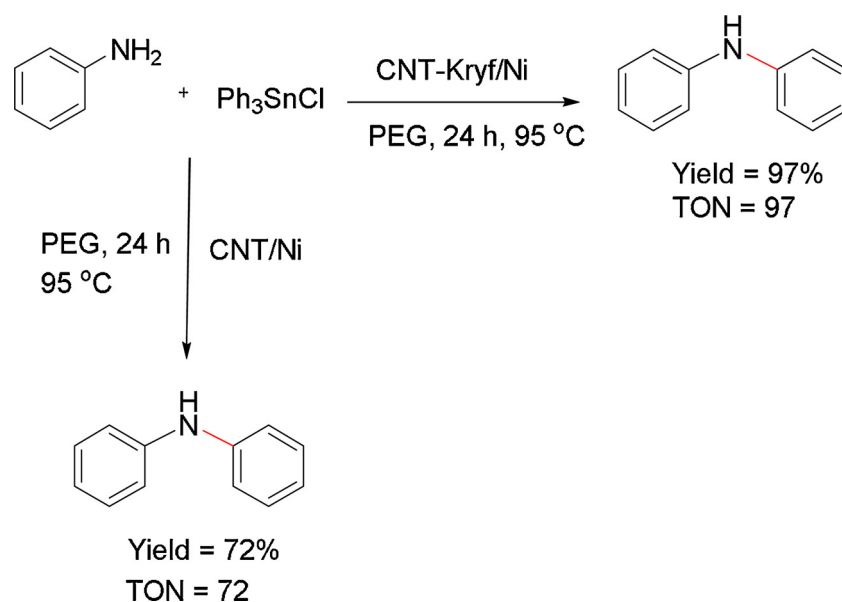
Further, we carried out a hot filtration test for the synthesis of C–C coupling reaction as a sample reaction with triphenyltin chloride and aryl bromide in order to examine the leaching of nickel to the reaction mixture and the heterogeneity of the catalyst. In this test, we filtered the catalyst in 20th minutes of the reaction and allowed the reaction continue. Afterward, the we observed no change in the progress of the reactions. This observation shows that there is no leached Ni^{2+} in the solution after filtration which is why the reaction progress was stopped (Fig. 7). We also observed the morphology and shape of recovered CNT/Kryf/Ni and we realised that the catalyst has been unchanged

Table 4
Coupling of phenol derivatives with Ph_3SnCl catalysed by CNT-Kryf/Ni at 90 °C.

Entry	Phenol	Product ^a	Yield (%) ^b	TON
1			94	94
2			96	96
3			87	87
4			84	84
5			92	92
6			89	89

^a The products were identified and characterised by comparison of their spectral and physical data with those of authentic samples.

^b Isolated yield.



Scheme 4. C–N coupling reaction of aniline with Ph_3SnCl in the presence of CNT-Kryf/Ni or CNT/Ni as catalyst under the identical conditions. (Reaction conditions: 1 mmol aniline, 0.5 mmol of Ph_3SnCl and 2 mmol of Et_3N in 2 ml of solvent).

after seven cycles.

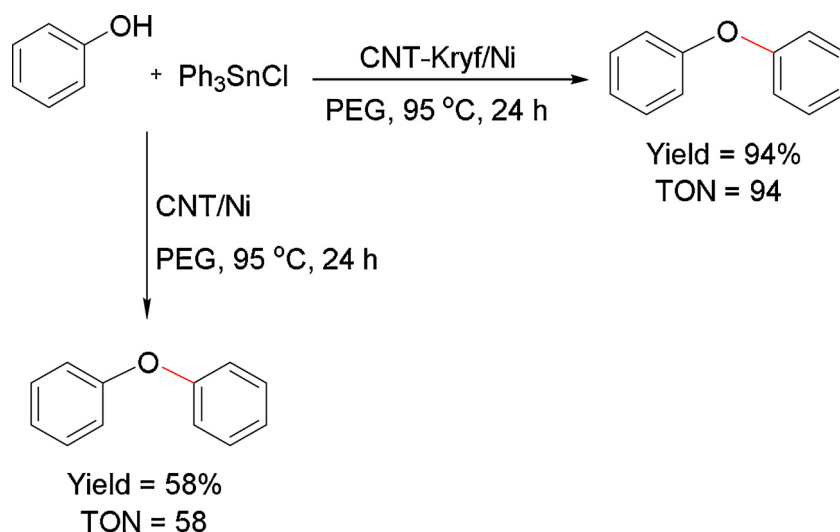
2.3. Conclusion

We demonstrated that kryptofix 22 can be a unique ligand for Ni^{2+} loading on the surface of CNT through a simple post modification process. Our proposed novel and retrievable catalyst (CNT-Kryf/Ni) revealed a promising catalytic activity in the C–C, CN and CO— cross-coupling reactions. Furthermore, the catalyst was active for several consecutive cycles without any leaching during the reaction. Our observations showed that this ligand on CNT has high potential to support a vast majority of cations that are resistive to surface adsorption.

3. Experimental

3.1. Materials and apparatus

All chemicals were purchased from Sigma-Aldrich and Merck companies. Nuclear magnetic resonance (NMR, 400 MHz) spectra were recorded on BRUKER NMR-Spectrometer (AVANCE). The FT-IR spectra were obtained with Nexus 670 FT-IR spectrometer. Thin layer chromatography (TLC) over silica gel SIL G/UV₂₅₄ plates were used to monitor the reactions progress. The amount of Ni loading was determined by ICP-OES (VISTA-PRO). N_2 adsorption–desorption isotherm and BET plot were obtained by a Quantachrome Autosorb at 77 K. XRD patterns were prepared using a Rigaku X-ray diffractometer equipped with a Cu radiation source. SEM observation and elemental SEM-EDS analysis were carried out with FESEM-TESCAN MIRA3.



Scheme 5. Cross coupling reaction of phenol with Ph_3SnCl through the catalysis of CNT-Kryf/Ni and CNT/Ni under the identical conditions. (Reaction conditions: 1 mmol phenol, 0.5 mmol of Ph_3SnCl and 2 mmol of Et_3N in 2 ml of solvent).

Table 5

Comparison of C–C, CO and CN— coupling reaction with CNT-Kryf/Ni and other reported systems.

Reaction type	Catalyst	Solvent	Temp. ($^\circ\text{C}$)	t (h)	Yield (%)	Ref.
C–C coupling	$\text{Pd(II)L}^{\text{a}}$	PEG	90	0.5	68	[39]
	$\text{Pd(II)L}^{\text{b}}$	H_2O	100	1	100	[40]
	CNT-Kryf/Ni	PEG	r.t.	1.5	97	This work
C–O coupling	CuI , DMG ^c	Dioxane	90	16	86	[41]
	Cu(OAc)_2	DMSO	120	20	86	[42]
	CNT-Kryf/Ni	PEG	95	18	94	This work
C–N coupling	Cu-L^{d}	H_2O	r.t.	15	91	[43]
	Cu(OAc)_2	Et_3N	r.t.	24	94	[42]
	CNT-Kryf/Ni	PEG	95	11	97	This work

^a L: *trans*-dichlorobis(triphenylphosphine).

^b L': Benzothiazole-based ligand.

^c *N,N* dimethylglycine.

^d L'': *N,N*-bis(salicylidene)arylmethanediamin.

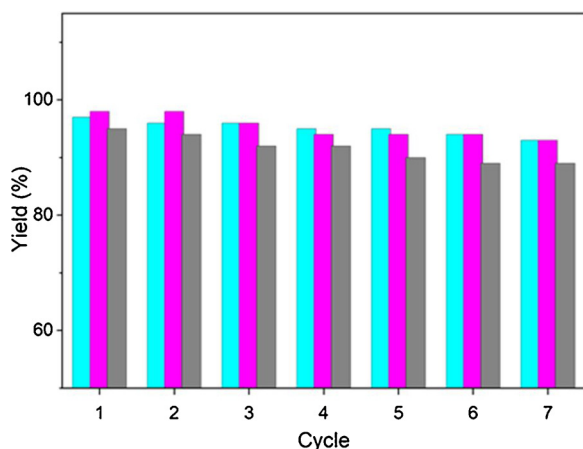


Fig. 6. Reusability of the CNT-Kryf/Ni C–C coupling (Purple), C–O (black), and C–N coupling (blue) reactions. (For interpretation of the references to colour in this figure legend, the reader is referred to the web version of this article).

3.2. Synthesis of CNT-Kryf/Ni

Multiwall CNT (2 g) was pretreated with concentrated $\text{H}_2\text{SO}_4/\text{HNO}_3$ mixture (9.0 M for each acid) and sonicated at $70\text{ }^\circ\text{C}$ for 3 h. The acid-treated CNT (4.8 g) was further dispersed in in toluene/CPTMS (10 mL, 5 mmol) solution and stirred at reflux conditions for 48 h. Then, the obtained powder from the reaction was recovered by centrifugation and washed with EtOH for three times. The obtained product from this step (CNT-Cl, 1 g) was added to kryptofix 22 (1 g) and Et_3N (2 mL) in EtOH (50 mL) and stirred under reflux for 24 h in a 100 ml round-bottom flask. Thus, the product (kryptofix 22/ MWCNTs) was filtered and washed by dry ethanol and dried in vacuum oven at $70\text{ }^\circ\text{C}$. In the final step, CNT-Kryf (3 g) was mixed with $\text{Ni(NO}_3)_2$ (1.5 g) in ethanol (50 mL) was stirred under reflux for 20 h. The CNT-Kryf/Ni was separated by filtration and washed with ethanol and dried in vacuum at $70\text{ }^\circ\text{C}$.

3.3. General procedure for C–C, CO and C–N couplings

–For CC coupling, aryl halide (1 mmol) was added to mixture of triphenyltin chloride (Ph_3SnCl , 0.5 mmol), K_2CO_3 (2 mmol) and CNT-Kryf/Ni (7 mg), and PEG (5 ml) at room temperature and stirred. The progress of the reaction was monitored by TLC. After reaction completion, the mixture was centrifuged to separate the catalyst. The recovered catalyst was then washed with water and ethanol for three times for next cycles (3:2, 5 mL). The reaction residue was diluted with chloroform and water, the extracted organic layer was dried with MgSO_4 and the solvent was vaporised to afford the product. The products were determined with gas chromatography a Shimadzu GC-2010 plus gas chromatograph equipped with a barrier ionisation discharge (BID) detector.

For C–O coupling, phenol (1 mmol), triphenyltin chloride (0.5 mmol) and Et_3N (2 mmol) in PEG (2 ml) were added to CNT-Kryf/Ni (7 mg) and the mixture was stirred at $95\text{ }^\circ\text{C}$, the progress of the reaction being monitored using TLC. After reaction completion, the mixture was centrifuged to separate the catalyst. The mixture was washed with water and EtOAc (3×5 ml), and then the separated organic layer was dried over MgSO_4 .

For C–N coupling, aniline (1 mmol), triphenyltin chloride (0.5 mmol) and Et_3N (2 mmol) in PEG (2 ml) was added CNT-Kryf/Ni (7 mg) at $95\text{ }^\circ\text{C}$. The progress of the reaction was monitored by TLC. The catalyst was separated by filtration and reused as such for the next experiment. The mixture was washed with water and EtOAc (3×5 ml), and then the separated organic layer was dried over MgSO_4 and solvent

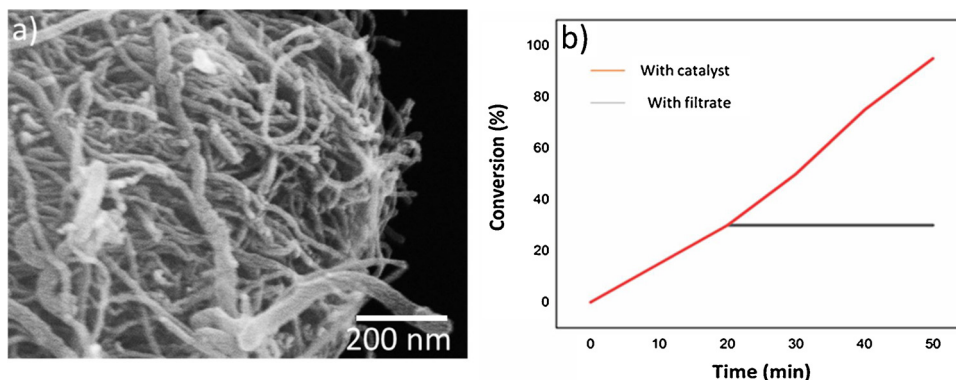


Fig. 7. a) SEM image of CNT-Kryf/Ni recovered from C–C cross coupling reaction after seven consecutive cycles; b) Hot filtration test profile for C–C coupling reaction.

was vaporised to provide the product.

CRedit author statement

Michael Aalinejad: Writing the draft, Conceptualization, Experiments; characterizations

Nader Noroozi-Pesyan: Supervision, revising the manuscript;

Esmail Doustkhah: Revising the draft, supervision, conceptualization.

Declaration of Competing Interest

The authors declare that they have no known competing financial interests or personal relationships that could have appeared to influence the work reported in this paper.

Acknowledgment

The authors are thankful for the financial support of Urmia University on accomplishment of the current project.

References

- [1] D.R. Rolison, *Science* 299 (2003) 1698–1701.
- [2] E. Doustkhah, J. Lin, S. Rostamnia, C. Len, R. Luque, X. Luo, Y. Bando, K.C.-W. Wu, J. Kim, Y. Yamauchi, Y. Ide, *Chem. Eur. J.* 25 (2019) 1614–1635.
- [3] H. Karimi-Maleh, O.A. Arotiba, J. Colloid Interface Sci. 560 (2020) 208–212.
- [4] M.H.N. Assadi, V. Sahajwalla, *Chem. Phys.* 443 (2014) 107–111.
- [5] E. Doustkhah, M. Hasani, Y. Ide, M.H.N. Assadi, *ACS Appl. Nano Mater.* 3 (2020) 22–43.
- [6] E. Doustkhah, H. Mohtasham, M. Hasani, Y. Ide, S. Rostamnia, N. Tsunaji, M. Hussein, N. Assadi, *Mol. Catal.* 482 (2020) 110676.
- [7] P. Kutudila, R. Linguerrri, M. Ponce-Vargas, C. Pichon, S. Condon, M. Hochlaf, *Mol. Catal.* 482 (2020) 110649.
- [8] C. Leal Marchena, G. Pecchi, L. Pierella, *Mol. Catal.* 482 (2020) 110685.
- [9] M. Esmat, A.A. Farghali, S.I. El-Dek, M.H. Khedr, Y. Yamauchi, Y. Bando, N. Fukata, Y. Ide, *Inorg. Chem.* 58 (2019) 7989–7996.
- [10] Y. Wu, X. Song, S. Xu, T. Yu, J. Zhang, Q. Qi, L. Gao, J. Zhang, G. Xiao, *Mol. Catal.* 475 (2019) 110485.
- [11] H. Pan, Y. Peng, X. Lu, J. He, L. He, C. Wang, F. Yue, H. Zhang, D. Zhou, Q. Xia, *Mol. Catal.* 485 (2020) 110838.
- [12] E. Doustkhah, H. Mohtasham, M. Farajzadeh, S. Rostamnia, Y. Wang, H. Arandiyani, M.H.N. Assadi, *Microporous Mesoporous Mater.* 293 (2020) 109832.
- [13] A.C. Villagrán-Olivares, M.F. Gomez, M.N. Barroso, M.C. Abello, *Mol. Catal.* 481 (2020) 110164.
- [14] A.R.O. Ferreira, J. Silvestre-Albergo, M.E. Maier, N.M.P.S. Ricardo, C.L. Cavalcante, F.M.T. Luna, *Mol. Catal.* 488 (2020) 110888.
- [15] E. Pérez-Mayoral, V. Calvino-Casilda, E. Soriano, *Catal. Sci. Technol.* 6 (2016) 1265–1291.
- [16] A. Şenocak, A. Khataee, E. Demirbas, E. Doustkhah, *Sens. Actuators B Chem.* 312 (2020) 127939.
- [17] Y. Liu, H. Zhang, Y. Dong, W. Li, S. Zhao, J. Zhang, *Mol. Catal.* 483 (2020) 110707.
- [18] E. Doustkhah, Y. Ide, *ACS Appl. Nano Mater.* 2 (2019) 7513–7520.
- [19] S. He, W. Wang, Z. Shen, G. Li, J. Kang, Z. Liu, G.-C. Wang, Q. Zhang, Y. Wang, *Mol. Catal.* 479 (2019) 110610.
- [20] H. Karimi-Maleh, M. Shafieizadeh, M.A. Taher, F. Opoku, E.M. Kiarri, P.P. Govender, S. Ranjbari, M. Rezapour, Y. Orooji, J. Mol. Liq. 298 (2020) 112040.
- [21] Y. Shen, M. Ge, A.C. Lua, *Catal. Sci. Technol.* 8 (2018) 3853–3862.
- [22] M. Li, F. Xu, H. Li, Y. Wang, *Catal. Sci. Technol.* 6 (2016) 3670–3693.
- [23] Y. Chen, H. Wang, S. Ji, R. Wang, *Catal. Commun.* 107 (2018) 29–32.
- [24] L.J. Konwar, P. Mäki-Arvela, J.-P. Mikkola, *Chem. Rev.* 119 (2019) 11576–11630.
- [25] J. Li, Q. Ren, L. Liu, K. Sun, X. Gu, *Mol. Catal.* 470 (2019) 97–103.
- [26] A. Vogler, *Inorg. Chem. Commun.* 51 (2015) 78–79.
- [27] G.H. Rounaghi, M. Gholizadeh, F. Moosavi, I. Razavipanah, H. Azizi-Toupkanloo, M.R. Salavati, *RSC Adv.* 6 (2016) 9096–9105.
- [28] D.J. Darensbourg, M. Pala, *J. Am. Chem. Soc.* 107 (1985) 5687–5693.
- [29] A. Mohadesi, M.A. Taher, F. Majidi, *J. Anal. Chem.* 66 (2011) 207–211.
- [30] A.G. Coman, C. Stavarache, A. Paun, C.C. Popescu, N.D. Hädade, P. Ionita, M. Matache, *RSC Adv.* 9 (2019) 6078–6083.
- [31] H. Fazelirad, M.A. Taher, *Environ. Technol.* 37 (2016) 300–307.
- [32] M.M. Dutta, P. Phukan, *Catal. Commun.* 109 (2018) 38–42.
- [33] Z.-L. Wu, H. Yang, F.-P. Jiao, Q. Liu, X.-Q. Chen, J.-G. Yu, *Colloids Surf. A* 470 (2015) 149–160.
- [34] F.M. Machado, C.P. Bergmann, T.H.M. Fernandes, E.C. Lima, B. Royer, T. Calvete, S.B. Fagan, *J. Hazard. Mater.* 192 (2011) 1122–1131.
- [35] X. Tian, J. Lin, S. Zou, J. Lv, Q. Huang, J. Zhu, S. Huang, Q. Wang, *J. Organomet. Chem.* 861 (2018) 125–130.
- [36] L. Ramin, M.H.N. Assadi, V. Sahajwalla, *J. Anal. Appl. Pyrolysis* 110 (2014) 318–321.
- [37] M.H.N. Assadi, V. Sahajwalla, *Ind. Eng. Chem. Res.* 53 (2014) 3861–3864.
- [38] E. Doustkhah, S. Rostamnia, M. Imura, Y. Ide, S. Mohammadi, C.J.T. Hyland, J. You, N. Tsunaji, B. Zeynizadeh, Y. Yamauchi, *RSC Adv.* 7 (2017) 56306–56310.
- [39] A. Naghipour, A. Ghorbani-Choghamarani, H. Babae, M. Hashemi, B. Notash, *J. Organomet. Chem.* 841 (2017) 31–38.
- [40] K.M. Dawood, M.R. Shaaban, M.B. Elamin, A.M. Farag, *Arabian J. Chem.* 10 (2017) 473–479.
- [41] D. Ma, Q. Cai, *Org. Lett.* 5 (2003) 3799–3802.
- [42] N. Iranpoor, H. Firouzabadi, E. Etemadi Davan, A. Rostami, A. Nematollahi, *J. Organomet. Chem.* 740 (2013) 123–130.
- [43] H. Batmani, N. Noroozi Pesyan, F. Havasi, *Appl. Organomet. Chem.* 32 (2018) e4419.